Hearing Research xxx (2017) 1–7

Contents lists available at ScienceDirect

Hearing Research

journal homepage: www.elsevier.com/locate/heares

Research Paper

Amplitude modulation rate dependent topographic organization of the auditory steady-state response in human auditory cortex

Nathan Weisz [a, b, *], Chrysoula Lithari [a, b]

[a] University of Trento, Center for Mind/Brain Sciences, Trento, Italy
[b] Paris-Lodron Universität Salzburg, Centre for Cognitive Neuroscience and Division of Physiological Psychology, Salzburg, Austria

ARTICLE INFO

Article history:
Received 4 April 2017
Received in revised form
6 August 2017
Accepted 8 September 2017
Available online xxx

Keywords:
Auditory steady-state response
Auditory cortex
Amplitude modulation
Magnetoencephalography
Beamforming

ABSTRACT

Periodic modulations of an acoustic feature, such as amplitude over a certain frequency range, leads to phase locking of neural responses to the envelope of the modulation. Using electrophysiological methods this neural activity pattern, also called the auditory steady-state response (aSSR), is visible following frequency transformation of the evoked response as a clear spectral peak at the modulation frequency. Despite several studies employing the aSSR that show, for example, strongest responses for ~40 Hz and an overall right-hemispheric dominance, it has not been investigated so far to what extent within auditory cortex different modulation frequencies elicit aSSRs at a homogenous source or whether the localization of the aSSR is topographically organized in a systematic manner. The latter would be suggested by previous neuroimaging works in monkeys and humans showing a periodotopic organization within and across distinct auditory fields. However, the sluggishness of the signal from these neuroimaging works prohibit inferences with regards to the fine-temporal features of the neural response. In the present study, we employed amplitude-modulated (AM) sounds over a range between 4 and 85 Hz to elicit aSSRs while recording brain activity via magnetoencephalography (MEG). Using beamforming and a fine spatially resolved grid restricted to auditory cortical processing regions, our study revealed a topographic representation of the aSSR that depends on AM rate, in particular in the medial-lateral (bilateral) and posterior-anterior (right auditory cortex) direction. In summary, our findings confirm previous studies that showing different AM rates to elicit maximal response in distinct neural populations. They extend these findings however by also showing that these respective neural ensembles in auditory cortex actually phase lock their activity over a wide modulation frequency range.

1. Introduction

Apart from spectral content, temporal amplitude modulations (i.e. derived from the temporal envelope of the signal) constitute an important feature of naturally occurring sounds. An example par excellence is speech, where diverse relevant acoustic features exhibit characteristic modulation rates (Kraus et al., 2000). Of particular importance for the intelligibility of speech appears to be the syllabic rate at ~3–6 Hz corresponding to the neural theta frequency range. Furthermore, higher frequencies in the low gamma range (~30 Hz) have been linked to phonemic processing. Using an amplitude modulated (AM) sound that shifted its modulation frequency across time, Lehongre et al. (2011) were able to show abnormal left-hemispheric processing in a group of dyslexia patients. Underlining the functional relevance of these measures of the brain's ability to follow rhythmic auditory information, the authors reported correlations with deficits in linguistic performance. Another relevant example in which acoustic rhythms play an outstanding role is music (Levitin et al., 2012). Based on observations that relevant acoustic rhythms strongly overlap in their frequency ranges with relevant neural rhythms, a functional link by which perceptual performance can be optimized has been suggested (Giraud and Poeppel, 2012). This is putatively implemented by neural rhythms which provide the auditory system with temporally predictable time windows for sampling the acoustic environment (Arnal and Giraud, 2012). Next to this sensory aspect the rhythmic structure of acoustic stimuli also enables strong integration with the motor system (Fujioka et al., 2009), which shares strong connections to auditory processing regions (Kraus

* Corresponding author. Paris-Lodron Universität Salzburg, Centre for Cognitive Neuroscience, Hellbrunnerstrasse 34, 5020 Salzburg, Austria.
E-mail address: nathan.weisz@sbg.ac.at (N. Weisz).

http://dx.doi.org/10.1016/j.heares.2017.09.003
0378-5955/

and White-Schwoch, 2015). In particular, the idea is gaining increased attention in cognitive neuroscience under the label of "entrainment", which posits the brain to align temporal high/low excitability phases to (predictable) periods of relevant/irrelevant sensory input respectively.

However, as compared to spectral organization, little is known about the organization of temporal modulations in auditory cortex. An early magnetoencephalography (MEG) study by Langner et al. (1997) hinted at a topographical organization of periodicity in auditory cortex, that was orthogonal to tonotopic representation. This rather crude spatial estimate which used a single moving dipole approach was supported and detailed by later animal neuroimaging studies that illustrated a topographical organization of modulation rates in auditory cortex. In particular, a recent study in awake macaques studying BOLD responses using a 4.7T MRI, Baumann et al. (2015) were able to identify modulation rate (studied between 0.5 and 128 Hz) dependent gradients along the superior temporal plane: while high modulation rates elicited maximal activation in posterior-medial (core) auditory regions, low rates elicited maximal activation in anterior core as well as lateral belt regions of auditory cortex. In humans, while it is generally accepted that sensitivity to faster modulation rates decreases along the ascending auditory system (~2–4 kHz at the level of the auditory nerve to max. 100–200 Hz in auditory cortex; see e.g. (Wallace et al., 2002)), the issue of topographical organization of modulation rates in the auditory cortex is less developed. Using fMRI and modulation rates between 4 and 128 Hz, Giraud et al. (2000) were unable to find a systematic spatial organization of modulation rates, which is in contrast to the macaque work. In another fMRI study, Herdener et al. (2013) observed a spatial organization, in particular along the medial-lateral axis, with higher AM rates being localized more towards medial parts of the auditory cortex. Similar to the macaque work (Baumann et al., 2015), representation of AM rates was orthogonal to the tonotopic organization (see also (Barton et al., 2012)).

A clear disadvantage of the aforementioned studies is that investigating the sluggish BOLD response does not allow to assess to what extent relevant neural populations indeed track AM rates by aligning their activity to the temporal envelope of the acoustic stimulus. These temporal features of neural responses are much better captured using electrophysiological techniques. A classical approach applies rhythmic sensory stimulation to elicit a so-called steady state response (Galambos, 1980). In the auditory modality, the steady-state response (aSSR) appears to elicit a maximum response in auditory cortex at ~40 Hz with a right-sided lateralization (Ross et al., 2005). However, whether the aSSR also exhibits a topographical representation, as suggested by the aforementioned fMRI studies, is not conclusively known. This was also not shown by the classically cited MEG study by Langner et al. (1997), which focused its analysis on low pass filtered transient evoked responses, in particular the M100, M200 and the sustained field. Liégeois-Chauvel et al. (2004) investigated the aSSR in epilepsy patients implanted with stereotactic electrodes, but were unable to identify clear modulation rate dependent spatial gradients. However, it could be argued that the spatial sampling with electrodes was insufficient to uncover fine spatially distributed patterns. In a noninvasive electrophysiological work using electroencephalography (EEG) and a predefined source montage, Herdmann et al. (Herdman et al., 2002) reported that aSSRs driven by a modulation frequency of 39 Hz have generators dominantly in primary auditory cortex (this finding is in line with several other reports also using alternative approaches; see e.g. (Draganova et al., 2007)). A faster modulation at 88 Hz elicits maximum responses in the brainstem, which is conform with the notion outlined previously that the capacity of auditory cortex to track faster amplitude modulations decreases. . In a recent study Farahani et al. (2017) also show responses that suggest aSSRs outside of the classical auditory pathway. However, the approaches in the described studies do not allow for any conclusions regarding a systematic spatial organization pattern for the different modulation frequencies along the supratemporal plane.

The goal of the present work was to elucidate the existence of a topographic organization of amplitude modulation rates in human auditory cortex as captured using the aSSR. By using beamforming applied to MEG data on a spatially fine (2 mm) grid and eliciting aSSRs with modulation frequencies between 4 and 85 Hz, we are able to show a spatial organization along the superior temporal plane, in particular in the medial-alteral and anterior-posterior direction very similar to previously published human and primate fMRI studies (Baumann et al., 2015).

2. Material and methods

2.1. Participants

Nineteen participants took part in the experiment (11 females; mean age: 29.4, SD: ±5 years). All participants reported normal hearing and absence of previous or current psychiatric or neurological problems. All participants gave written informed consent before the experiment. The procedure was approved by the Ethics Committee of the University of Trento.

2.2. Stimuli and procedure

Auditory stimuli were generated in Matlab (MathWorks, Natick, MA) at a sampling rate of 44.1 kHz. For this purpose, a 200 kHz tone of 3 s duration was amplitude modulated (100% modulation depth) at seven different rates: 4, 10, 15, 25,40, 65 and 85 Hz. Stimuli were binaurally presented at an ambient intensity level via air-conducting tubes with ear inserts (SOUNDPixx, VPixx technologies, Canada). Every AM frequency was presented 80 times, pseudo-randomly distributed over four measurement blocks. Intertrial intervals were jittered uniformly between 2 and 4 s. During sound presentation, participants watched a silent movie.

2.3. Data acquisiton

MEG recordings were obtained at a sampling rate of 1 kHz using a 306-channel (204 first order planar gradiometers, 102 magnetometers) VectorView MEG system (Elekta-Neuromag Ltd., Helsinki, Finland) in a magnetically shielded room (AK3B, Vakuumschmelze, Hanau, Germany). Before the experiment, individual head shapes were acquired for each participant including relevant anatomical landmarks (nasion, pre-auricular points) and around 200 digitized points on the scalp with a Polhemus Fastrak digitizer (Polhemus, Vermont, USA). Head positions of the individuals relative to the MEG sensors were continuously controlled using five coils. Head movements did not exceed 1.5 cm within and between blocks.

2.4. Data analysis and statistics

Data were analyzed offline using the Fieldtrip toolbox (Oostenveld et al., 2011). First, a high-pass filter at 1 Hz (6th order Butterworth IIR) was applied on continuous data. Then, trials of 1 s pre- and 4 s post-stimulus were extracted and trials containing physiological or acquisition artifacts were rejected (average number of rejected trials per condition: 6.55; range across all conditions: 0–17). The number of trials were equalized across the seven conditions for each subject to ensure that our results were not confounded by systematic differences in signal-to-noise ratio

Please cite this article in press as: Weisz, N., Lithari, C., Amplitude modulation rate dependent topographic organization of the auditory steady-state response in human auditory cortex, Hearing Research (2017), http://dx.doi.org/10.1016/j.heares.2017.09.003

(average number of trials retained in analysis: 69.84; range across participants: 63–74). Bad channels were excluded from the whole data set (average number of rejected sensors: 6.84; range across participants: 4–10). Sensor space trials were projected into source space using linearly constrained minimum variance beamformer filters (Van Veen et al., 1997) and further analysis was performed on the obtained time-series of each brain voxel. Since structural MRIs were available only for few participants, we decided to use a template MRI in the Fieldtrip toolbox, that were morphed to the individual head shape in MEG space using affine transformation. The aligned brain volumes were also used to create single-sphere head models and lead field matrices (Nolte, 2003). Using a grid in MNI space warped to the individual anatomy allowed us to average and compute statistics since each grid point in the warped grid, despite different space coordinates, belongs to the same brain region across participants. For the creation of this template grid we chose a resolution of 2 mm in MNI space. Furthermore, using the Brainnetome atlas (http://atlas.brainnetome.org), we restricted the placement of grid points to primary and secondary auditory regions, in particular along the superior temporal gyrus (STG) for the left and right hemisphere respectively (7304 grid points per hemisphere, 14,608 in total). These areas are depicted in Fig. 1A. The average covariance matrix (calculated for a period between 0 and 3 s), the head model and the lead field matrix were used to calculate a common beamformer filter for all conditions. The filters were subsequently multiplied with the sensor space trials, resulting in source space trials (see www.fieldtriptoolbox.org/tutorial/shared/virtual_sensors). To estimate the aSSR at the different AM frequencies two strategies were used. In one approach time-series of trials belonging to each AM condition were averaged separately to derive an evoked response. This averaged signal was then entered into a time-frequency analysis, estimating power at each AM frequency using FFTs calculated on time windows of 0.5 s (hanning-tapered) shifted between −0.5 and 4 s in steps of 0.05 s. The time-resolved evoked power at each AM was subsequently baseline normalized using a pre-sound time-window of −0.3 to −0.1 s, to obtain changes of power in decibel (dB). In a second approach time-frequency analysis using the identical parameters for the evoked response was applied to the single-trial time-series. Using the complex valued Fourier spectra, we then calculated for each AM condition separately the so-called Inter-Trial Phase Coherence (ITPC), a measure that describes the phase consistency across trials (Delorme and Makeig, 2004). Analogous to evoked power, ITPC was baseline normalized using a pre-sound time-

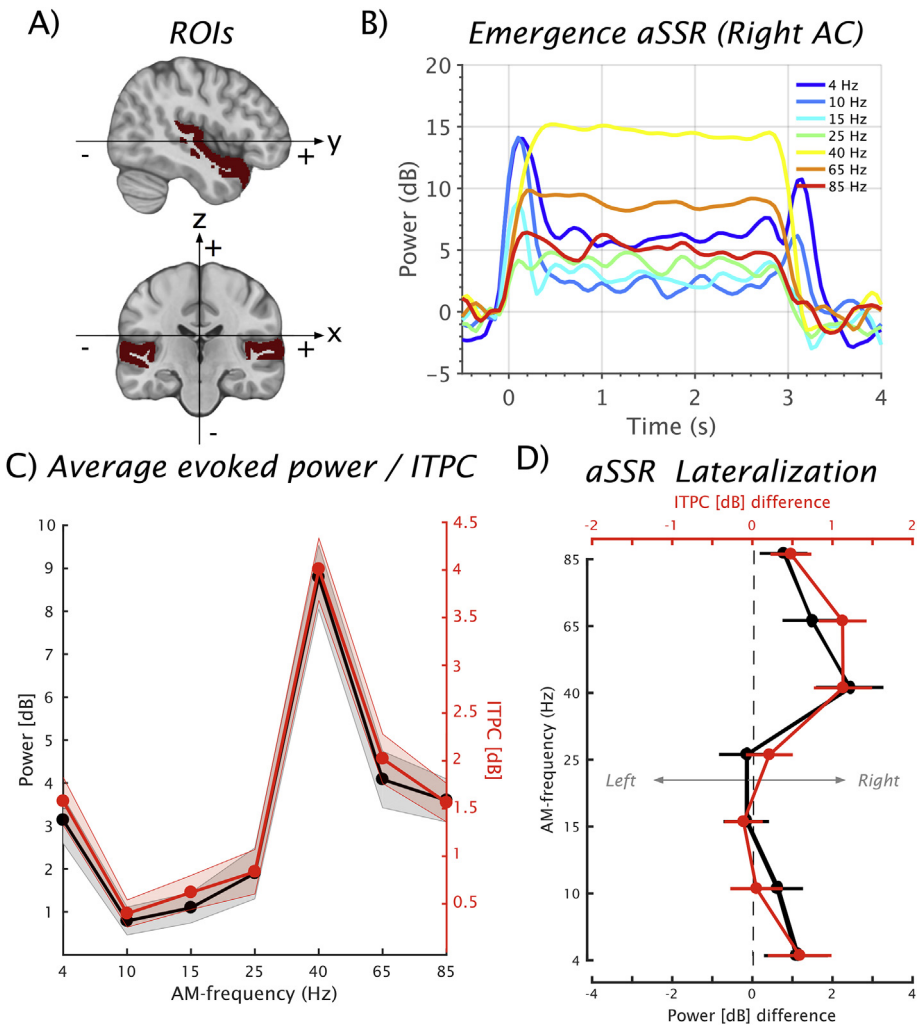

Fig. 1. a) Bilateral regions of the STG according to the Brainnetome atlas. b) Temporal evolution of the aSSR (evoked power) at different modulation rates. c) Evoked power and ITPC averaged between 0.4 and 2.9 s following sound onset shows the established maximum response at ~40 Hz. d) Lateralization of the aSSR evoked power and ITPC showed an overall effect towards the right hemisphere. Post-hoc analysis showed that this effect was particularly pronounced for the 40 Hz AM and –for ITPC also- 65 Hz, albeit only at an uncorrected level.

Please cite this article in press as: Weisz, N., Lithari, C., Amplitude modulation rate dependent topographic organization of the auditory steady-state response in human auditory cortex, Hearing Research (2017), http://dx.doi.org/10.1016/j.heares.2017.09.003

window of −0.3 to −0.1 s, to obtain changes in decibel (dB).

To assess the validity and data quality of our study, one part of the analysis pertained to replicating previously reported effects: such as the maximum evoked power for AMs around 40 Hz (Draganova et al., 2007) and the stronger right lateralization of the aSSR (Ross et al., 2005). To this end, evoked power and ITPC values were averaged over a time-window in which aSSRs appeared relatively stable (0.4–2.9 s) and values (left - right in the case of the laterality analysis) were entered into a repeated measures ANOVA, followed up by post-hoc testing using *Tukey's Honestly Significant Difference* procedure (implemented in Matlab's *multcompare* function). For our main analysis, namely the topographic organization of AM rates, peak location along the x-, y- and z-axis for the three highest and three lowest frequencies within the 0.4 to 2.9 s period were averaged separately for each hemisphere and participant. These average locations were compared using paired sample t-tests in x, y and z direction to yield a coarse hint at potential peridotopic organization (see Fig. 1A for directions). In a more rigorous test targeting the spatial organization of AM rates we determined for each individual, separately for AM frequency and hemisphere, the peak location along the x-, y- and z-axis. To assess linear relationships between the AM rates and spatial location on each axis, we used a robust regression method (the *rlm* function implemented in R using default parameters; https://cran.r-project.org/web/packages/rlm/rlm.pdf) and extracted the respective regression coefficient. The coefficients were averaged across individuals to yield an empirically observed regression coefficient for each hemisphere and spatial axis. To test for statistical significance, we implemented a permutation test in which the sequence of AM rates was randomly shuffled and the robust regression recalculated. This was repeated 1000 times to obtain a distribution of mean regression coefficients for each hemisphere and spatial axis. This allowed the determination of the probability of observing the empirically determined average regression coefficient under the H0, assuming no topographic relationship between AM rate and spatial location. Since this test was performed in a two-sided manner separately for each hemisphere and spatial axis, only probabilities surviving Bonferroni-correction (i.e. at both sides of the distribution more extreme than $(0.05/2)/6 = 0.0042$) are considered as significant. While evoked power and ITPC yielded comparable results, in this manuscript we restrict the description of the topographic organization of the aSSR to ITPC.

3. Results

3.1. ASSR emergence and laterality

AM sounds elicited reliable evoked responses reflecting the modulation frequency, namely so-called aSSRs. Exemplary evoked power time courses are depicted for auditory cortical ROIs (see Fig. 1A) in Fig. 1B, descriptively showing for all frequencies the robust emergence of a SSR following ~200 ms after sound onset and lasting for the duration of stimulation. The depiction also shows that, on average, strongest aSSRs are obtained at 40 Hz, which conforms to previous reports. This overall impression is confirmed by the statistical analysis performed over an averaged time-window of .4–2.9 s (see Fig. 1C). A repeated measures ANOVA results in a highly significant effect for modulation frequency results for evoked power ($F_{6,108} = 20.87$, $p < 0.001$) as well as for ITPC ($F_{6,108} = 23.35$, $p < 0.001$). Post-hoc testing using Tukey's HSD shows, as expected for evoked power and for ITPC, that the aSSR elicited by the 40 Hz AM sound is significantly stronger than the aSSR of all other AM sounds (all p's < 0.007). Further, for evoked both 65 Hz and 85 Hz aSSRs were more pronounced than those recorded for the 10 Hz and 15 Hz AM sounds (all p's < 0.05). The same was the case for ITPC with the exception of the 65 vs 15 Hz AM sound, which did not survive multiple comparison testing. Finally, the aSSR observed for the 4 Hz AM sound was stronger than the respective response to the 10 Hz sound for evoked power ($p < 0.03$) as well as ITPC ($p < 0.009$). We also investigated whether the AM sounds lead to lateralized responses, the outcome of which is shown in Fig. 1D. While on a descriptive level it appears as if higher AM frequencies (≧40 Hz) elicited more right-lateralized aSSRs, a repeated measures ANOVA could not find a significant difference between AM frequencies neither for evoked power ($F_{6,108} = 1.45$, $p = 0.2$) nor for ITPC ($F_{6,108} = 2.09$, $p = 0.06$). A highly significant effect was found for the intercept (evoked power: $F_{1,18} = 8.93$, $p = 0.008$; ITPC: $F_{1,18} = 11.11$, $p = 0.004$), implying an overall lateralization of aSSRs towards the right auditory cortex. Following up on this effect using a one-sample *t*-test of the lateralization value against 0 points to a significant right-lateralization, in particular for the 40 Hz AM sound ($p_{\text{uncorrected}} = 0.02$) in case of evoked power and 40 an 65 Hz AM sound in case of ITPC ($p_{\text{uncorrected}} = 0.02$ and 0.007 respectively). While this observation is well in line with previous reports (Ross et al., 2005), only the 65 Hz AM sound ITPC effect survises correction for multiple comparison using fdr ($p_{\text{corrected}} = 0.046$).

3.2. Topographic organization of AM frequency in auditory cortex

The main goal of the current study was to assess to which degree different rates of AM frequencies engage auditory cortex in a topographical manner, as has been previously reported in monkeys (Baumann et al., 2015). Since ITPC lead to similar findings as evoked power and appeared somewhat more robust overall (e.g. clearer lateralization effect; see Fig. 1), this analysis was continued with ITPC. Extracting the peak coordinates for each individual AM frequency in the left and right ROI descriptively suggests the presence of a topographical organization (see Fig. 2A): in both hemispheres the faster AM rates (≥40 Hz) peaked in more posterior regions as compared to the slower AM rates (≤ 15 Hz; difference right hemisphere ~ −1.1 cm, $t_{18} = -4.67$, $p < 0.001$; difference left hemisphere ~ −0.94 cm, $t_{18} = -3.11$, $p = 0.006$). Another clear effect, conforming to the aforementioned literature, was observed on the medial-lateral axis, with higher AM rates being localized more medially (difference right hemisphere ~ −0.79 cm, $t_{18} = -3.9$, $p = 0.001$; difference left hemisphere ~ −0.59 cm, $t_{18} = 2.76$, $p = 0.01$). Furthermore, conforming with the anatomical organization of the superior temporal plane being more elevated at posterior sites (see Fig. 1A), higher AM frequencies overall lead to more superior localized maxima than slower AM frequencies. This effect was significant however only for the left auditory cortex (~0.88 cm, $t_{18} = 3.61$, $p = 0.005$) and reached trend level in the right auditory cortex (~0.66 cm, $t_{18} = 1.87$, $p = 0.08$). Relating the mean position for slow and fast AM rates to the Brainnetome atlas, points to slow AM rates (≤ 15 Hz) enganging predominantly more belt regions of the auditory cortex (BA22), faster AM rates (≥40 Hz) seem to engage predominantly core regions of the auditory cortex (BA41 and 42; Te1.0 and Te1.2). While these analyses are very suggestive of a topographical organization of AM rates, we implemented a more rigorous testing procedure, using the location information from all AM frequencies to compute the relationship using robust regression in each individual and tested the significance of the mean regression coefficient using a permutation test (see Fig. 2B). This analysis underlines the aforementioned relationship between AM frequency and peak location for the posterior-anterior direction in the right hemisphere, with the negative coefficient indicating a more posterior localization of higher A. A similar trend was also obtained for the left hemisphere, however the coefficient did not exceed the rigorous threshold given by Bonferroni correction (middle panel of Fig. 2B). Concerning the medial-lateral direction,

Please cite this article in press as: Weisz, N., Lithari, C., Amplitude modulation rate dependent topographic organization of the auditory steady-state response in human auditory cortex, Hearing Research (2017), http://dx.doi.org/10.1016/j.heares.2017.09.003

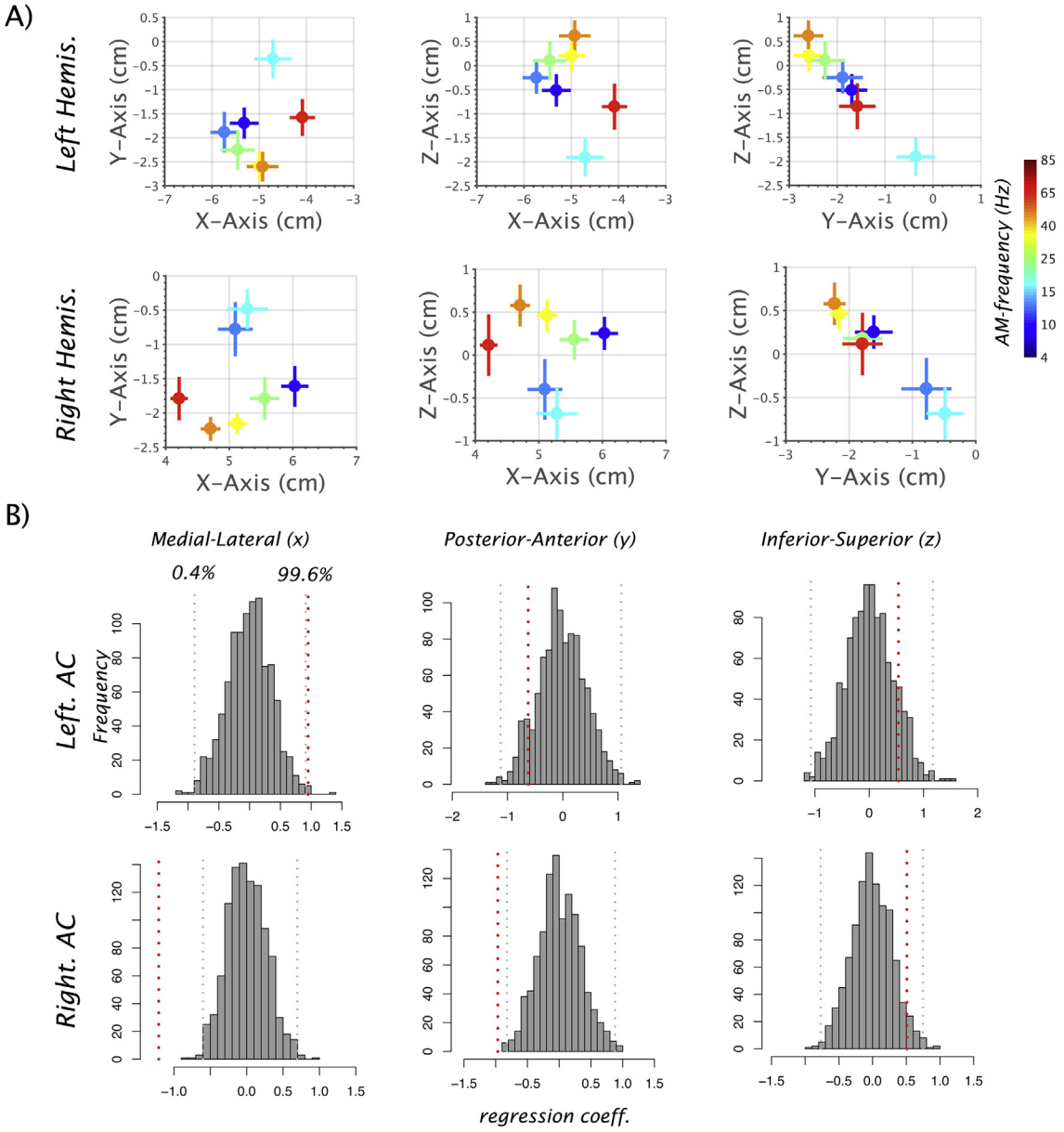

Fig. 2. a) Points representing grand averaged Cartesian coordinates (error bars representing standard error of mean) color-coded for different AM rates based on ITPC. c) Robust regression between AM rate and location in x-, y- and z-direction for each individual subject indicates a significant relationship in the posterior-anterior direction for the right hemisphere and in the medial-lateral direction for both hemispheres. Significance was determined by comparing empirically observed (mean) regression coefficients (red dotted lines) with a distribution of (mean) regression coefficients obtained from 1000 permutations. Grey dotted lines represent thresholds given by Bonferroni correction. (For interpretation of the references to colour in this figure legend, the reader is referred to the web version of this article.)

clear effects were observed in both hemispheres, with regression coefficients suggesting a more medial localization of higher AM frequencies (note that positive and negative coefficients imply more medial locations of high AM frequencies in left and right auditory cortex respectively). With respect to the inferior-superior direction, while both hemispheres exhibited, on average, positive coefficients, namely more superior locations of higher AM frequencies, the effect was not significant at a Bonferroni-corrected level (see right panel of Fig. 2B).

4. Discussion

The goal of the present study was to assess to what extent processing of AM rate in auditory cortex as assessed via the aSSR follows a topographic representation. It may be noted that while the *resolution* of MEG is insufficient to resolve simultaneously active sources in close vicinity, the *accuracy* of isolated peak locations for stimuli presented in isolation could be sufficient to estimate periodotopic gradients. Indeed, a previous MEG study (Langner et al., 1997) on six individuals illustrated spatial gradients according to periodicity of the acoustic stimulus. Yet to the best of our knowledge no study thus far has reported a systematic spatial arrangement for the aSSR. This is of particular interest, since neither these transient evoked responses, nor the sluggish responses as captured using fMRI actually allow for conclusions as to whether the spatially resolved neural activity patterns track the temporal envelope of the acoustic stimulus in a faithful manner, that is, by phase locking its respective activity. Also, the aforementioned study by Langner et al. (1997) used complex tones to elicit periodicities $\geq$ 50 Hz, temporal modulations that can go along

Please cite this article in press as: Weisz, N., Lithari, C., Amplitude modulation rate dependent topographic organization of the auditory steady-state response in human auditory cortex, Hearing Research (2017), http://dx.doi.org/10.1016/j.heares.2017.09.003

with clear perception of pitch, which, however, are beyond the slower AM rates that carry important information, for example, for speech comprehension (Kraus et al., 2000). Here, we used seven AM frequencies between 4 and 85 Hz and applied beamforming to MEG data using a grid with 2 mm resolution, focusing on areas along the STG. Using evoked power as well as ITPC, our analysis confirmed relevant, previously reported aSSR effects, such as the relative maximum for AM rates of 40 Hz and the overall right lateralization of the aSSR (Ross et al., 2005; Draganova et al., 2007). While in particular our lateralization finding (Fig. 1D) is fully conform with the aforementioned aSSR literature, it is interesting to point out that the popular asymmetric sampling in time hypothesis (Poeppel, 2003) proposes a left auditory cortical dominance of gamma rhythms and a right auditory cortical dominance of theta rhythms. This is supported among other things by hemispheric differences in resting state rhythms (Giraud et al., 2007). This may seem contradictory to our findings, however these works usually make strong claims with regards to endogenous rhythms. Also, the empirical situation regarding this hypothesis is not straight-forward (see e.g. Millman et al., 2011). We do not aim to make any links or claims between the rhythms evoked by phase-locking of neural responses to the amplitude envelope and endogenous rhythm.

Our most important finding is the topographic organization of the aSSR depending on AM rate, especially in the anterior-posterior direction auditory cortices in both hemispheres when comparing high vs low AM rates and for the right hemisphere using our nonparametric permutation test of regression coefficients. A strong topographic organization of AM rates was also identified in the medial-lateral direction of both auditory cortices. Overall, faster AM rates lead to aSSRs located in more posterior and medial parts of the STG, whereas slower AM rates peaked at more anterior and lateral locations. The general trend aligns well with a recent monkey study (Baumann et al., 2015), as well as human fMRI studies (Barton et al., 2012; Herdener et al., 2013); however, the spatial resolution in the current study is too limited to make claims for subfields of the auditory cortex. This is not only due to basic limitations of the technique with regards to localization, but also due to the fact that we decided to use a template anatomy for all participants since structural data was largely missing. This will lead to inaccuracies of the headmodel and by extension the resolution of our localization will suffer to some extent. Despite these methodological limitations, when grouping over different AM rates, faster modulation rates lead to maxima more in primary auditory regions (BA 41/42) as compared to slower modulation rates that overall more located in secondary auditory regions (BA22). Based on these results, it is likely that different AM rates engage auditory fields (core and belt regions) of auditory cortex in a differential manner. This finding is in line with animal electrophysiology showing a decreased synchronization of more rostral regions of the auditory cortex, in particular, to faster AM rates (Bendor and Wang, 2008). These effects may in part be due to timing advantages of neural responses of more caudal auditory regions as compared to rostral regions, that could belong to dorsal and ventral auditory streams respectively (Camalier et al., 2012). However, to investigate to what extent these animal works reflect similar processes as observed in our study would require high spatially-resolved invasive mapping of the aSSR in animals. One potential aspect that could contribute to the presented findings is that the faster periodicities (>30 Hz) used in the present study could be accompanied by a distinct perception of pitch (or roughness, when individual beats are not anymore perceived), which would be absent for the lower AM rates (when individual beats are still perceived. While this is theoretically possible, it does not seem to fit with current ideas of dedicated pitch processing areas, which would suggest a more lateral localization (Bendor and Wang, 2006); however, increasing AM rate and putatively sensation of pitch does not show any tendency in the medial-lateral axis along these lines. On the contrary, higher AM rates appear to elicit stronger aSSRs in medial portions of the auditory cortex. Nevertheless, the relationship of our patterns to perceptual features is a complex issue, that cannot be conclusively addressed based on our results. Also, in the current study, we cannot make any claims of a potential orthogonal representation of tonotopy as compared to AM rate of the aSSR, since only a single carrier frequency was used here (as mentioned previously, the work by Langner et al. (1997) did not study the aSSR). A previous MEG study by Wienbruch et al. (Wienbruch et al., 2006; see also Pantev et al., 1996) suggests that the spatial gradients for carrier frequency may be similar to those observed in our study for AM rate. Next to a tonotopic gradient in the posterior-anterior and inferior-superior direction, the authors also report an overall more medial localization of 40 Hz AM aSSRs with higher carrier frequencies. This would be somewhat in contradiction to aforementioned neuroimaging works (Barton et al., 2012; Herdener et al., 2013; Baumann et al., 2015) which showed an orthogonal organization of AM rates to tonotopy. Upcoming M/EEG studies similar to ours should therefore parametrically manipulate the carrier frequency next to the AM rate. Finally, we want to point out that our approach of using (robust) linear regressions, gives a coarse “global” relationship between AM rate and maximum (ITPC) location. Naturally, this is a great simplification and indeed our results hint at the true complexities in periodotopic organization (see Fig. 2A) that will be partially driven by individual factors (e.g. anatomical organization) as well as interindividual variability.

Taken together, we show for the first time a topographic organization of the aSSR to varying AM rates, especially in the posterior-anterior direction and medial-lateral. While being in line with previous works, our results illustrate that spatially separate neural populations in auditory cortex faithfully track the temporal envelope of the stimulus by phase locking their activity accordingly.

Acknowledgements

This work was supported by the European Research Council (grant number 28304). We thank Carolina Sánchez-Garcia for her support.

References

Arnal, L.H., Giraud, A.-L., 2012. Cortical oscillations and sensory predictions. Trends Cogn. Sci. 16, 390–398.
Barton, B., Venezia, J.H., Saberi, K., Hickok, G., Brewer, A.A., 2012. Orthogonal acoustic dimensions define auditory field maps in human cortex. Proc. Natl. Acad. Sci. 109, 20738–20743.
Baumann, S., Joly, O., Rees, A., Petkov, C.I., Sun, L., Thiele, A., Griffiths, T.D., 2015. The topography of frequency and time representation in primate auditory cortices. Elife 4, e03256.
Bendor, D., Wang, X., 2006. Cortical representations of pitch in monkeys and humans. Curr. Opin. Neurobiol. 16, 391–399.
Bendor, D., Wang, X., 2008. Neural response properties of primary, rostral, and rostrotemporal core fields in the auditory cortex of marmoset monkeys. J. Neurophysiol. 100, 888–906.
Camalier, C.R., D'Angelo, W.R., Sterbing-D'Angelo, S.J., Lisa, A., Hackett, T.A., 2012. Neural latencies across auditory cortex of macaque support a dorsal stream supramodal timing advantage in primates. Proc. Natl. Acad. Sci. 109, 18168–18173.
Delorme, A., Makeig, S., 2004. EEGLAB: an open source toolbox for analysis of single-trial EEG dynamics including independent component analysis. J. Neurosci. methods 134, 9–21.
Draganova, R., Ross, B., Wollbrink, A., Pantev, C., 2007. Cortical steady-state responses to central and peripheral auditory beats. Cereb. Cortex 18, 1193–1200.
Farahani, E.D., Goossens, T., Wouters, J., van Wieringen, A., 2017. Spatiotemporal reconstruction of auditory steady-state responses to acoustic amplitude modulations: potential sources beyond the auditory pathway. Neuroimage 148, 240–253.
Fujioka, T., Trainor, L.J., Large, E.W., Ross, B., 2009. Beta and gamma rhythms in

Please cite this article in press as: Weisz, N., Lithari, C., Amplitude modulation rate dependent topographic organization of the auditory steady-state response in human auditory cortex, Hearing Research (2017), http://dx.doi.org/10.1016/j.heares.2017.09.003

human auditory cortex during musical beat processing. Ann. N. Y. Acad. Sci. 1169, 89–92.
Galambos, R., 1980. Tactile and auditory stimuli repeated at high rates (30–50 per sec) produce similar event related potentials. Ann. N. Y. Acad. Sci. 338, 722–726.
Giraud, A.-L., Lorenzi, C., Ashburner, J., Wable, J., Johnsrude, I., Frackowiak, R., Kleinschmidt, A., 2000. Representation of the temporal envelope of sounds in the human brain. J. Neurophysiol. 84, 1588–1598.
Giraud, A.-L., Kleinschmidt, A., Poeppel, D., Lund, T.E., Frackowiak, R.S., Laufs, H., 2007. Endogenous cortical rhythms determine cerebral specialization for speech perception and production. Neuron 56, 1127–1134.
Giraud, A.-L., Poeppel, D., 2012. Cortical oscillations and speech processing: emerging computational principles and operations. Nat. Neurosci. 15, 511–517.
Herdener, M., Esposito, F., Scheffler, K., Schneider, P., Logothetis, N.K., Uludag, K., Kayser, C., 2013. Spatial representations of temporal and spectral sound cues in human auditory cortex. Cortex 49, 2822–2833.
Herdman, A.T., Lins, O., Van Roon, P., Stapells, D.R., Scherg, M., Picton, T.W., 2002. Intracerebral sources of human auditory steady-state responses. Brain Topogr. 15, 69–86.
Kraus, N., Bradlow, A.R., Cheatham, M.A., Cunningham, J., King, C.D., Koch, D.B., Nicol, T.G., McGee, T.J., Stein, L.K., Wright, B.A., 2000. Consequences of neural asynchrony: a case of auditory neuropathy. J. Assoc. Res. Otolaryngol. 1, 33–45.
Kraus, N., White-Schwoch, T., 2015. Unraveling the biology of auditory learning: a cognitive–sensorimotor–reward framework. Trends Cogn. Sci. 19, 642–654.
Langner, G., Sams, M., Heil, P., Schulze, H., 1997. Frequency and periodicity are represented in orthogonal maps in the human auditory cortex: evidence from magnetoencephalography. J. Comp. Physiol. A Neuroethol. Sens. Neural, Behav. Physiol. 181, 665–676.
Lehongre, K., Ramus, F., Villiermet, N., Schwartz, D., Giraud, A.-L., 2011. Altered low-gamma sampling in auditory cortex accounts for the three main facets of dyslexia. Neuron 72, 1080–1090.
Levitin, D.J., Chordia, P., Menon, V., 2012. Musical rhythm spectra from Bach to Joplin obey a 1/f power law. Proc. Natl. Acad. Sci. 109, 3716–3720.
Liégeois-Chauvel, C., Lorenzi, C., Trébuchon, A., Régis, J., Chauvel, P., 2004. Temporal envelope processing in the human left and right auditory cortices. Cereb. Cortex 14, 731–740.
Millman, R.E., Woods, W.P., Quinlan, P.T., 2011. Functional asymmetries in the representation of noise-vocoded speech. Neuroimage 54, 2364–2373.
Nolte, G., 2003. The magnetic lead field theorem in the quasi-static approximation and its use for magnetoencephalography forward calculation in realistic volume conductors. Phys. Med. Biol. 48, 3637.
Oostenveld, R., Fries, P., Maris, E., Schoffelen, J.M., 2011. FieldTrip: open source software for advanced analysis of MEG, EEG, and invasive electrophysiological data. Comput. Intell. Neurosci. 2011, 156869.
Pantev, C., Roberts, L.E., Elbert, T., Ross, B., Wienbruch, C., 1996. Tonotopic organization of the sources of human auditory steady-state responses. Hear Res. 101, 62–74.
Poeppel, D., 2003. The analysis of speech in different temporal integration windows: cerebral lateralization as 'asymmetric sampling in time'. Speech Commun. 41, 245–255.
Ross, B., Herdman, A.T., Pantev, C., 2005. Right hemispheric laterality of human 40 Hz auditory steady-state responses. Cereb. Cortex 15, 2029–2039.
Van Veen, B.D., Van Drongelen, W., Yuchtman, M., Suzuki, A., 1997. Localization of brain electrical activity via linearly constrained minimum variance spatial filtering. IEEE Trans. Biomed. Eng. 44, 867–880.
Wallace, M.N., Shackleton, T.M., Palmer, A.R., 2002. Phase-locked responses to pure tones in the primary auditory cortex. Hear. Res. 172, 160–171.
Wienbruch, C., Paul, I., Weisz, N., Elbert, T., Roberts, L.E., 2006. Frequency organization of the 40-Hz auditory steady-state response in normal hearing and in tinnitus. Neuroimage 33, 180–194.

Please cite this article in press as: Weisz, N., Lithari, C., Amplitude modulation rate dependent topographic organization of the auditory steady-state response in human auditory cortex, Hearing Research (2017), http://dx.doi.org/10.1016/j.heares.2017.09.003